ACS APPLIED MATERIALS & INTERFACES

Research Article

www.acsami.org

Ultrathin Transparent Conductive Polyimide Foil Embedding Silver Nanowires

Dhriti Sundar Ghosh,*[,†] Tong Lai Chen,*[,†] Vahagn Mkhitaryan,[†] and Valerio Pruneri[†,‡]

[†]ICFO—Institut de Ciencies Fotoniques, Mediterranean Technology Park, Av. Carl Friedrich Gauss, 3, 08860 Castelldefels, Barcelona, Spain

[‡]ICREA—Institució Catalana de Recerca i Estudis Avançats, 08015 Barcelona, Spain

Supporting Information

ABSTRACT: Metallic nanowires are among the most promising transparent conductor (TC) alternatives to widely used indium tin oxide (ITO) because of their excellent trade-off between electrical and optical properties, together with their mechanical flexibility. However, they tend to suffer from relatively large surface roughness, instability against oxidation, and poor adhesion to the substrate. Embedding in a suitable material can overcome these shortcomings. Here we propose and demonstrate a new TC comprising silver nanowires (AgNWs) in an ultrathin polyimide foil that presents an optical transmission in the visible larger than ITO (>90%), while maintaining similar electrical sheet resistance (15 ohm/sq). The polyimide protects the Ag against environmental agents such as oxygen and water and, thanks to its deformability and very small thickness (5 μm), provides an ideal mechanical support to the NW's network, in this way ensuring extreme flexibility (bending radius as small as at least 1 mm) and straightforwardly removing any adhesion issue. The initial AgNWs' roughness is also reduced by a factor of about 15, reaching RMS values as low as 2.4 nm, suitable for the majority of applications. All these properties together with the simple fabrication technique based on all-solution processing put the developed TC in a competitive position as a lightweight, mechanically flexible and inexpensive substrate for consumer electronic and optoelectronic devices.

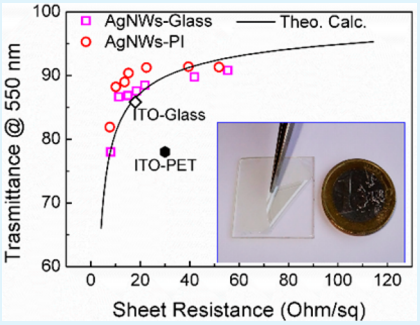

KEYWORDS: *silver nanowires, polyimide, solution processed, mechanical flexibility, transparent conductors*

INTRODUCTION

Thin film transparent conductors (TCs) that combine high electrical conductivity and optical transmittance are of great importance to electronic and photonic devices, in particular, photovoltaic cells, touch-screen displays, and organic light emitting diodes. Apart from low electrical sheet resistance (R_S) and high optical transmittance (T_{OPT}), the durability and compatibility with large scale manufacturing are also essential features for ensuring commercialization of the final products containing the TCs.[1,2] In addition, with the emergence of flexible optoelectronic devices, the next generation of TCs should be capable of withstanding significant bending.[3,4] Until now, indium tin oxide (ITO) is the most widely used TC thanks to its advantageous trade-off between T_{OPT} and R_S. However, on one hand, the shortage of indium makes ITO expensive while, on the other hand, the fact that thick oxide layers (typically of the order of 100 nm) are fragile and easily crack under bending makes ITO unsuitable for roll-to-roll processing (R2R) of polymeric flexible devices,[5,6] which is becoming essential for low cost production of flexible electronic and optoelectronic devices.

There has thus been a widespread search for new flexible TC materials and geometries such as graphene,[3,7] carbon nanotubes,[8] metal grids,[9,10] random metal nanowires,[11,12] conducting polymers,[13] and their combinations.[14−16] However, apart from metal grids and nanowires, most of these TCs suffer from poor electrical conductivity resulting in devices with low efficiency. Metallic nanowires (NWs), especially those made of silver (Ag), have somehow emerged from other ITO alternatives, especially when one considers the trade-off between T_{OPT} and R_S. In particular, devices incorporating Ag NWs based TCs have been shown to perform as well as those with ITO.[17,18] However, the high surface roughness and their poor adhesion to the substrates are major drawbacks that still need to be addressed in an effective manner.[19] Usually, NW films are obtained by either spin coating,[14,16] Meyer rod,[12] dry transfer,[20] Doctor Blade method,[21] or spray coating.[22] These methods lead to NWs dispersed on the substrate surface without an efficient contact between them and with the substrate itself. As a consequence, the NWs can easily detach from the substrate, for example even after a weak smudge or blowing low pressure air/N_2. Recently, to address the adhesion problem, nail-polish solution[23] and encapsulation by metal oxide colloidal solution have been used with some success.[14,24]

Polyimide (PI) possesses outstanding thermal/mechanical stability with a high glass transition temperature (>350 °C), light weight, chemical inertness, excellent mechanical properties, low thermal expansion coefficient, and also high tensile

Received: August 23, 2014
Accepted: November 13, 2014
Published: November 13, 2014

strength.[25,26] It has already been used as high performance substrate in microelectronics and aerospace industries. In this work, we report a free-standing TC together with its enhanced properties, which is made of AgNWs directly embedded in a PI substrate using all solution processing methods. The resulting conductive substrate has T_{OPT} as high as >90% (550 nm) and R_S as low as 15 Ohm/sq; it is mechanically flexible, and presents a very smooth surface (2.4 nm root-mean-square value).

EXPERIMENTAL DETAILS

Electrode Fabrication. The fabrication steps for the proposed TC are schematically shown in Figure 1. Glass or polyethylene terephthalate (PET) (0.125 μm) substrates were cleaned in acetone followed by ethanol for 15 min using an ultrasonic bath. Commercially available AgNWs (average diameter in the 15−35 nm range; average length 15−30 μm; produced by Seashell Tech., California) were spin coated onto glass/PET substrates. Prior to spin coating, the AgNWs dispersed in IPA solution were diluted down to the required concentration (approximately 4.4 mg/mL). After a few minutes of drying at room temperature, a clear grade PI solution (VTEC-080051) is then spin coated onto AgNWs and is annealed, first at 100 °C for 10 min and subsequently at 180 °C for an additional 10 minutes. Annealing makes the PI dry and consequently solidify into a thin film. The PI incorporating the Ag NWs is then carefully peeled off from the glass/PET substrate, in this way creating a solid, smooth, and free-standing flexible TC (AgNW embedded PI: AgNW-PI) (Figure 2a,b). The thickness of the PI thin film can be controlled by adjusting the spin-coater speed. In this work, the thickness of the PI film was between 5 and 6 μm. Other techniques, such as Doctor Blade, Meyer rod, or spray coating methods could also be used to deposit the PI film on the top of AgNWs. The glass/PET substrate can be reused to deposit a new AgNW-PI film.

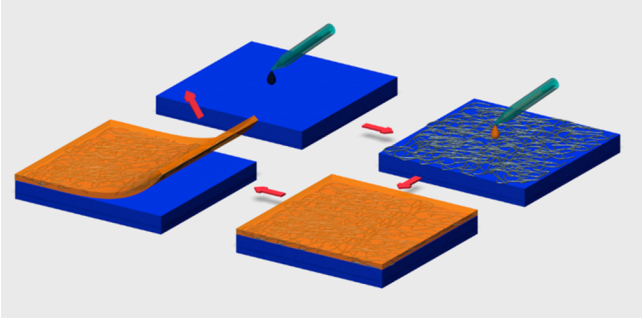

Figure 1. Fabrication steps of AgNW-PI transparent conductive substrate. AgNWs suspended in isopropanol were spin-coated onto a glass/plastic substrate. This was followed by spin coating of polyimide (PI). After annealing (100 °C for 10 min followed 180 °C for additional 10 min), the PI with embedded AgNWs was peeled off from the supporting glass/plastic substrate.

Electrical and Optical Characterization. The R_S measurements of the films were carried out by a Cascade Microtech 44/S 2749 four-point probe system with a Keithley 2001 multimeter. The results were cross checked with the van der Pauw method. Optical transmittance measurements were carried out by a PerkinElmer Lambda 950 UV−vis−NIR spectrophotometer.

Surface and Stability Characterization. Surface morphology was investigated by a digital instrument D3100 atomic force microscope (AFM) and FEI-scanning electron microscopy (SEM). The AFM image analysis was carried out with Nanoscope 7.30 software. A humidity chamber Vötsch VCL 7003 was used for the damp-heat test in harsh conditions of 85 °C and 85% relative humidity for a period of 30 days.

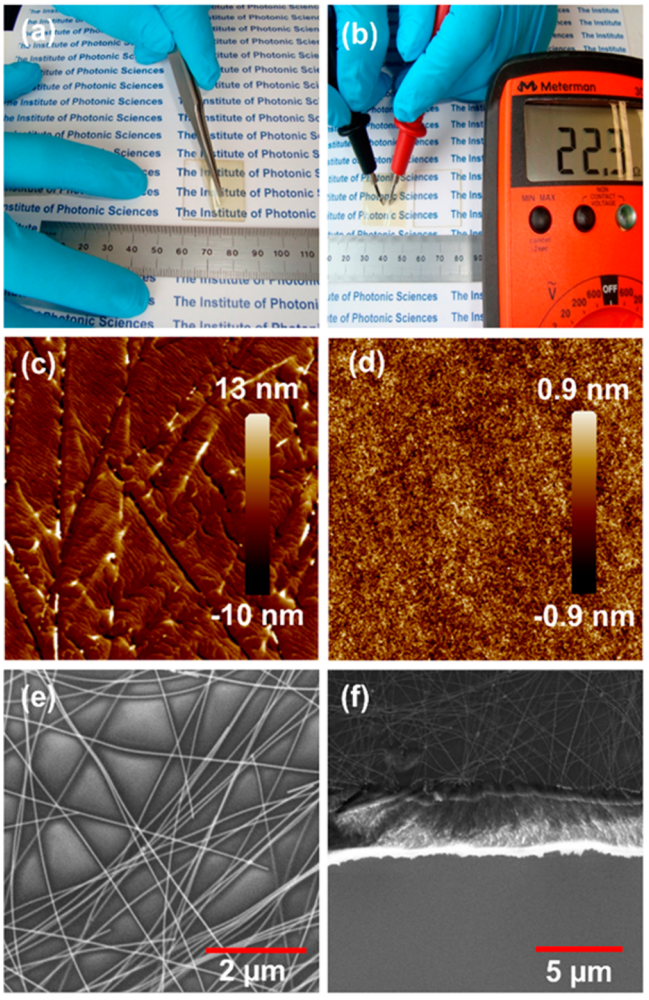

Figure 2. (a) Peeling-off of AgNW-PI transparent electrode from the glass substrate. (b) Resistance measurement showing electrical conduction. Atomic force microscope (AFM) images of front (c) and back side (d) of the AgNW-PI transparent conductor. Top (e) and cross-sectional (f) scanning electron microscope (SEM) images of the developed AgNW-PI structure.

Transparent Heater. A source fitted with potentiometer was used to apply the voltage. Temperature was recorded as a function of time using Fluke 566 infrared thermometer.

RESULTS AND DISCUSSION

Figure 2c−f shows the atomic force microscope (AFM) and scanning electron microscope (SEM) images of a typical AgNW-PI based TC. A root-mean-square (RMS) roughness of 2.4 and 0.2 nm was measured for the front side with AgNWs and back side, respectively. The smooth surface morphology clearly indicates that the AgNWs are partially embedded inside the PI film. AgNW films on bare glass show roughness larger than 35 nm which is considered one of the most critical parameters preventing them to be used in, for example, efficient organic photovoltaic cells without any buffer layers. In the case of pristine AgNW films, high morphological peaks (heights can easily exceed 80 nm) exist where NW overlaps, depending on the NW's diameter and density. The PI material tends to fill the gaps in between the NWs and reduce the overall roughness. Note that wrinkles can form on the front side during peeling off of the PI from the supporting glass/PET substrate, as is evident in the AFM images. The SEM images clearly show the presence

of PI in-between Ag NWs. In addition, the cross-section SEM image indicates that the Ag NWs are mainly localized on one side of the PI film (Figure 2f).

Figure 3 shows the T_{OPT} (at 550 nm) and R_S of different concentrations of AgNWs on both glass (□) and PI (○). As it

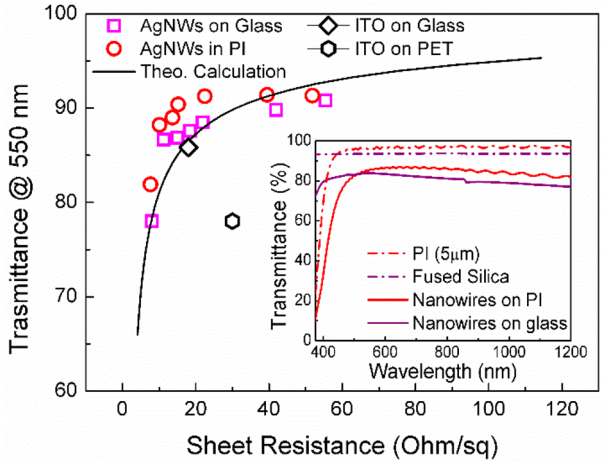

Figure 3. Optical transmittance at a wavelength of 550 nm as a function of electrical sheet resistance for the developed transparent conductor for different concentrations of AgNWs. The picture also shows theoretical calculated values of only AgNWs along with standard ITO values. The inset picture shows the transmittance spectra of AgNW-PI along with AgNW on glass, blank glass, and only polyimide (PI) film.

can be seen, the AgNW-PI films show higher transmission and slightly lower R_S for a given concentration. More detailed information regarding the change in R_S for AgNWs-PI films can be found in the Supporting Information (Figure S1). The reason for higher T_{OPT} is mainly due to the higher transmittance of bare PI films compared to blank glass substrate (inset of Figure 3). In fact, the glass substrate (UV fused silica) shows a flatter spectrum over the wavelength range of interest while PI film substrate has superior transmission except for the ultraviolet (UV) region. For comparison reasons, corresponding values for commercially available ITO on glass and PET are also shown. One can note that AgNWs both on glass and PI films present improved electro-optical performance trade-off with respect to ITO. In particular AgNW-PI shows significantly higher T_{OPT} and lower R_S compared to ITO on PET substrates, both of them being flexible.

The size and shape of the NWs lead to light scattering which is generally known as the haze effect. This effect, which can be significantly reduced by moving to lower NW diameters, if properly tailored, could lead to enhanced interaction and absorption with the active layer in a device.[24] The haze factor of the deposited AgNW-PI samples for different concentrations is measured to be in the range 1.2−3.5% (the higher the NW concentration the higher the haze). Thus, the AgNW-PI film presents comparable haze to AgNWs only on glass. The measured R_S values of all the samples ranged from 7.5 Ohm/sq to 52 Ohm/sq depending on the AgNW concentration. For the same concentration of AgNWs, the AgNW-PI films showed slightly better R_S compared to AgNWs only on glass. This can be explained in terms of the gradual drying of PI solution which provides the capillary forces for aggregating PI film around the NWs, thus increasing their contact and reducing the corresponding resistance.[27] The process of annealing itself also helps to decrease the contact resistance as it improves PI aggregation around the NWs.

For a AgNW mesh, the electrical R_S is usually related to T_{OPT} through either a percolation[28] or random walk theory.[29] The percolation model is governed by the equation

$$\frac{\sigma_e}{\sigma_m} = 1 + \frac{(1-\delta)\eta f}{3}\left(\frac{1}{\frac{\sigma_m}{\eta\sigma_3} + F(\eta p)}\right) + \frac{\delta\eta^2 f}{3}\left(\frac{\sigma_3}{\sigma_m}\right) \quad (1)$$

where σ_e is the effective electrical conductivity, σ_m is the electrical conductivity of the matrix in which NWs are embedded, η is denoting the straightness ratio of the NWs, and $\eta\sigma_3$ and ηf represent the nominal electrical conductivity and volume fraction, respectively. $F(\eta p)$ and δ, respectively, reflect the influence of the aspect ratio $p = L/d$ (L and d are NW length and diameter respectively), and the probability of percolation between the NWs.

The random walk model can be formulated as follows:

$$\sigma = \sigma_0 a\left\{1 - \frac{1}{2\sqrt{\ln\alpha}\frac{a}{b}}\tanh\left(2\sqrt{\ln\alpha}\frac{a}{b}\right)\right\} \quad (2)$$

Here $\sigma_0 h$ is the bare conductivity of an average conductive path, and a and b stand for the vertical distance between random walk steps and step length, respectively. α is a relative factor associated with a finite reduction in conductivity. By combining these two equations, we can reach a complete description of any nanowire network/mesh, with an ability to predict the percolation properties and also dependence of R_S on nanowire film thickness which is subsequently related to the T_{OPT} via the Beer−Lambert law. The solid curve in Figure 3 shows the calculated values along with the experimental values for different concentrations of AgNWs on both glass and PI.

In addition to the excellent electro-optical properties and smooth surface morphology, another advantage of the AgNW-PI films is its superior durability under mechanical stress, an essential property for making devices that is sometimes overlooked. To examine the flexibility properties of the developed TCs, both AgNW-PI and AgNW on PET were subjected to tensile bending with different radii of curvature, from 1 to 10 mm. Figure 4a shows the percentage change in R_S ($\Delta R_S/R_S$) of the films after 10 bending cycles for each of the decreasing radii of curvature. The AgNW-PI film showed negligible increase in resistance for small radii of curvature while this was more evident for AgNWs on PET film. More specifically, for 1 mm radius of curvature the change in resistance for AgNW-PI and AgNW-PET was about ∼1.0% and ∼2.8%, respectively. Note that the corresponding bending strains ($=t_s/2r$ where t_s is the substrate thickness and r is the radius of curvature) are 0.6% and 12.5%, respectively. The small thickness of the PI not only helps to reduce the overall weight of the embedded TC but also exhibits much less bending strain compared to thicker substrates for the same radius of curvature. A similar test on commercially available ITO (100 nm) on PET shows a >300% increase in R_S caused by its fragility and large thickness. The robustness of the AgNW-PI was also confirmed by the fact that it showed an R_S increase of ∼3.7% after 1000 bending cycles with 1 mm radius of curvature (inset Figure 4a). Under the same conditions, the AgNW on PET shows ∼10% increase while the ITO film has >500% increase only after 20 cycles. In addition, during the peeling off the film from the glass/PET substrate, the AgNW-PI film undergoes severe

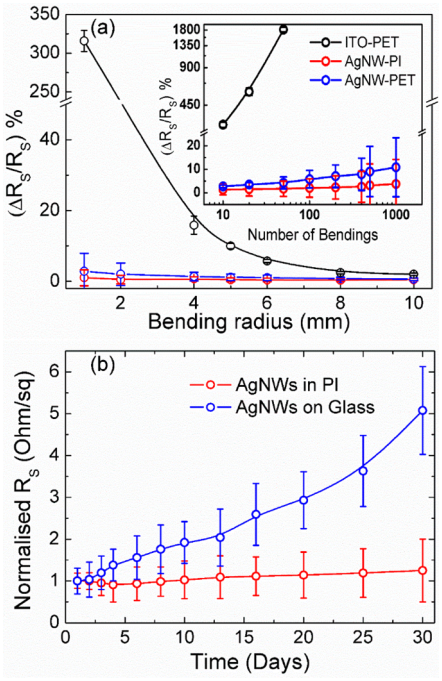

Figure 4. (a) Changes in electrical sheet resistance (R_S) during mechanical bending test, after 10 bending cycles as a function of radius curvature for AgNW-PI, ITO, and AgNW both on PET. Inset picture shows the performance of the AgNW-PI transparent conductive substrate for fixed radius of curvature (1 mm) as a function of bending cycles. (b) Evolution of sheet resistance of AgNW-PI and AgNW on glass during damp heat (85 °C and 85% relative humidity).

bending, and its low R_S is another confirmation of extreme robustness and excellent mechanical strength (see also Supporting Information Figure S2 and movies M1 and M2).

Another critical aspect of pristine NW on glass/PET is their adhesion to the substrate and, consequently, robustness to mechanical handling. For pristine AgNW films, the connection between NWs and their adhesion to substrate is primarily driven by gravity, van der Waals forces, and capillary forces from solvent (IPA) evaporation. Those forces cannot provide high strength, as is also confirmed by the fact that typically NWs can be easily removed by simply touching or finger sliding. On the contrary, AgNW-PI films show extreme mechanical strength to external mechanical manipulation, including the scotch tape test under which they did not show significant change in electro-optical properties.

The environmental and chemical stability of the AgNW-PI film was also investigated. The films were kept in standard damp heat conditions, at a temperature of 85 °C and relative humidity of 85%, and their electro-optical properties were periodically measured over 30 days (Figure 4b). The pristine AgNW film showed the highest (5 times) change in R_S, while the AgNW-PI film exhibited much smaller changes (1.2 times), indicating the expected protection of the PI matrix against oxidation and water corrosion of the AgNWs. We have also investigated the optical properties of the films during the damp heat. The optical spectrum of AgNWs-PI showed little change over a damp heat test period of 30 days while the bare AgNWs on glass showed reduced transmittance (Figure S3, Supporting Information). This behavior can be explained by the effective protection provided by the PI against environmental oxidation and corrosion of the NWs. The reduced transmittance of bare AgNWs on glass is also characterized by a plasmonic behavior at low wavelengths (300−370 nm) associated with the change in material composition, from metallic Ag to its oxide/sulfide, with this resulting in change of plasma frequency.

We demonstrated the functional potential of the proposed AgNW-PI film by fabricating a transparent thin-film heater (TTFH) based on the Joule's heating effect. TTFHs can be used for antifogging, anti-icing, and deicing of surfaces for displays, vehicle headlamps, traffic lights, windows, camera lenses, and touch-screens.[30−32] In this work, a TTFH was realized using a AgNW-PI film (area of 2.5 cm × 2.4 cm). The temperature was recorded for a given applied voltage during 60 s and then with voltage switched-off for additional 30 s. For a given applied voltage, the increase in temperature was fast and reached saturation (maximum temperature) after about 20 s. The higher the voltage is, the higher the maximum temperature (Figure 5). The uniformity of the heating element was

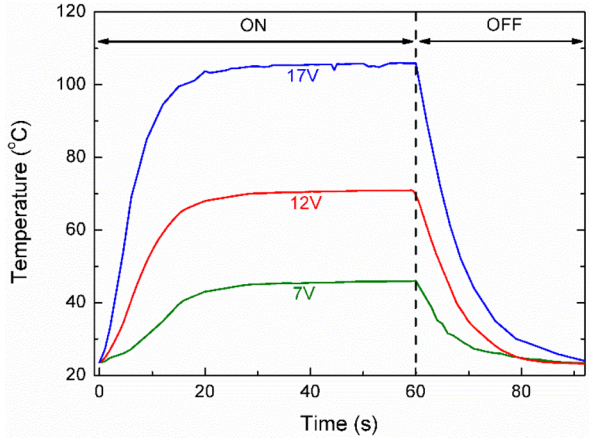

Figure 5. Temperature profiles as a function of time for AgNW-PI film having sheet resistance equal to 15 Ohm/sq at different applied voltages.

confirmed by measuring the temperature in different areas after saturation is reached. The maximum temperature was also recorded for different bending positions; the AgNW-PI film showed no change in temperature with respect to the flat configuration. This agrees with the measurements that showed unchanged electrical sheet resistance after bending.

CONCLUSIONS

In conclusion, we have developed a robust free-standing ultrathin TC made of AgNWs embedded in a PI film. Microscopy analysis showed that the PI fills the gaps in between the NWs, thus reducing the surface roughness more than 1 order of magnitude with respect to the AgNWs on a substrate (without PI embedding). The thin PI film is more transparent than a glass substrate, and the AgNW-PI structure exhibits an optical transmittance larger than 90% when the electrical sheet resistance is smaller than 15 ohm/sq. The mechanical strength and chemical stability of PI film provides support and protection to the NWs under bending and harsh environmental (e.g., humidity and temperature) conditions, making the combined structure very promising for flexible electronic and optoelectronic devices.

■ ASSOCIATED CONTENT

Supporting Information

More detailed information regarding the change in R_S for AgNWs-PI films. Detailed information regarding the change in electrical sheet resistance for AgNWs-PI films and the effect of damp heat test on optical properties. Evidence of mechanical robustness and surface conduction. Movies demonstrating film properties. This material is available free of charge via the Internet at http://pubs.acs.org.

■ AUTHOR INFORMATION

Corresponding Authors

*E-mail: dhriti.ghosh@icfo.es.

*E-mail: tonglai.chen@icfo.es.

Author Contributions

The manuscript was written through contributions of all authors. All authors have given approval to the final version of the manuscript.

Notes

The authors declare no competing financial interest.

■ ACKNOWLEDGMENTS

This work was partly supported by the Ministerio de Ciencia e Innovacion through Grant TEC 2010-14832. We also acknowledge financial support from the Spanish Ministry of Economy and Competitiveness (MINECO) and the "Fondo Europeo de Desarrollo Regional" (FEDER) through Grant TEC2013-46168-R. T.L.C. also acknowledges the financial support by the Ramon y Cajal (RyC) fellowship programme.

■ REFERENCES

(1) Hu, L.; Wu, H.; Cui, Y. Metal Nanogrids, Nanowires, and Nanofibers for Transparent Electrodes. *MRS Bull.* **2011**, *36*, 760−765.

(2) Ellmer, K. Past Achievements and Future Challenges in the Development of Optically Transparent Electrodes. *Nat. Photonics* **2012**, *6*, 809−817.

(3) Bae, S.; Kim, H.; Lee, Y.; Xu, X.; Park, J.-S.; Zheng, Y.; Balakrishnan, J.; Lei, T.; Kim, H. R.; Song, Y II; Kim, Y. J.; Kim, K. S.; Özyilmaz, B.; Ahn, J.-H.; Hong, B. H.; Iijima, S. Roll-to-roll Production of 30-in. Graphene Films for Transparent Electrodes. *Nat. Nanotechnol.* **2010**, *5*, 574−578.

(4) Hu, L.; Kim, H. S.; Lee, J.-Y.; Peumans, P.; Cui, Y. Scalable Coating and Properties of Transparent, Flexible, Silver Nanowire Electrodes. *ACS Nano* **2010**, *4*, 2955−2963.

(5) Ghosh, D. S.; Martinez, L.; Giurgola, S.; Vergani, P.; Pruneri, V. Widely Transparent Electrodes Based on Ultrathin Metals. *Opt. Lett.* **2009**, *34*, 325−327.

(6) Stec, H. M.; Williams, R.; Jones, T. S.; Hatton, R. A. Ultrathin Transparent Au Electrodes for Organic Photovoltaics Fabricated Using a Mixed Mono-Molecular Nucleation Layer. *Adv. Funct. Mater.* **2011**, *21*, 1709−1716.

(7) Wu, J.; Becerril, H. A.; Bao, Z.; Liu, Z.; Chen, Y.; Peumans, P. Organic Solar Cells with Solution-Processed Graphene Transparent Electrodes. *Appl. Phys. Lett.* **2008**, *92*, 263302.

(8) Pasquier, A. D.; Unalan, H. E.; Kanwal, A.; Miller, S.; Chhowalla, M. Conducting and Transparent Single-Wall Carbon Nanotube Electrodes for Polymer-Fullerene Solar Cells. *Appl. Phys. Lett.* **2005**, *87*, 203511.

(9) Kang, M.-G.; Kim, M.-S.; Kim, J.; Guo, L. J. Organic Solar Cells Using Nano-Imprinted Transparent Metal Electrodes. *Adv. Mater.* **2008**, *20*, 4408−4413.

(10) Ghosh, D. S.; Chen, T. L.; Pruneri, V. High Figure-of-Merit Ultrathin Metal Transparent Electrodes Incorporating a Conductive Grid. *Appl. Phys. Lett.* **2010**, *96*, 041109.

(11) De, S.; Higgins, T. M.; Lyons, P. E.; Doherty, E. M.; Nirmalraj, P. N.; Blau, W. J.; Boland, J. J.; Coleman, J. N. Silver Nanowire Networks as Flexible, Transparent, Conducting Films: Extremely High DC to Optical Conductivity Ratios. *ACS Nano* **2009**, *3*, 1767−1774.

(12) Hu, L.; Kim, H. S.; Lee, J.-Y.; Peumans, P.; Cui, Y. Scalable Coating and Properties of Transparent, Flexible, Silver Nanowire Electrodes. *ACS Nano* **2010**, *4*, 2955−2963.

(13) Schubert, S.; Kim, Y. H.; Menke, T.; Fischer, A.; Timmreck, R.; Meskamp, L. M.; Leo, K. Highly Doped Fullerene C60 Thin films as Transparent Standalone Top Electrode for Organic Solar Cells. *Sol. Energy Mater. Sol. Cells* **2013**, *118*, 165−170.

(14) Ghosh, D. S.; Chen, T. L.; Mkhitaryan, V.; Formica, N.; Pruneri, V. Solution Processed Metallic Nanowire Based Transparent Electrode Capped with a Multifunctional Layer. *Appl. Phys. Lett.* **2013**, *102*, 221111.

(15) Gaynor, W.; Burkhard, G. F.; McGehee, M. D.; Peumans, P. Smooth Nanowire/Polymer Composite Transparent Electrodes. *Adv. Mater.* **2011**, *23*, 2905−2910.

(16) Chen, T. L.; Ghosh, D. S.; Mkhitaryan, V.; Pruneri, V. Hybrid Transparent Conductive Film on Flexible Glass Formed by Hot-Pressing Graphene on a Silver Nanowire Mesh. *ACS Appl. Mater. Interfaces* **2013**, *5*, 11756−11761.

(17) Morgensten, F. S.; Kabra, D.; Massip, S.; Brenner, T. J. K; Lyons, P. E.; Coleman, J. N.; Friend, R. H. Ag-Nanowire Films Coated with ZnO Nanoparticles as a Transparent Electrode for Solar Cells. *Appl. Phys. Lett.* **2011**, *99*, 183307.

(18) Yu, Z.; Zhang, Q.; Li, L.; Chen, Q.; Niu, X.; Liu, J.; Pei, Q. Highly Flexible Silver Nanowire Electrodes for Shape-Memory Polymer Light-Emitting Diodes. *Adv. Mater.* **2011**, *23*, 664−668.

(19) Zeng, X.-Y.; Zhang, Q.-K.; Yu, R.-M.; Lu, C.-Z. A New Transparent Conductor: Silver Nanowire Film Buried at the Surface of a Transparent Polymer. *Adv. Mater.* **2010**, *22*, 4484−4488.

(20) Madaria, A. R.; Kumar, A.; Zhou, C. Large Scale, Highly Conductive and Patterned Transparent Films of Silver Nanowires on Arbitrary Substrates and their Application in Touch Screens. *Nanotechnology* **2011**, *22*, 245201.

(21) Padinger, F.; Brabec, C. J.; Fromherz, T.; Hummelen, J. C.; Sariciftci, N. S. Fabrication of Large Area Photovoltaic Devices Containing Various Blends of Polymer and Fullerene Derivatives by Using the Doctor Blade Technique. *Optoelectron. Rev.* **2000**, *4*, 280−283.

(22) Scardaci, V.; Coull, R.; Lyons, P. E.; Rickard, D.; Coleman, J. N. Spray Deposition of Highly Transparent, Low-Resistance Networks of Silver Nanowires over Large Areas. *Small* **2011**, *7*, 2621−2628.

(23) Liu, C.-H.; Yu, X. Silver Nanowire-Based Transparent, Flexible, and Conductive Thin Film. *Nanoscale Res. Lett.* **2011**, *6*, 75.

(24) Zhu, R.; Chung, C.-H.; Cha, K. C.; Yang, W.; Zheng, Y. B.; Zhou, H.; Song, T.-B.; Chen, C.-C.; Weiss, P. S.; Li, G.; Yang, Y. Fused Silver Nanowires with Metal Oxide Nanoparticles and Organic Polymers for Highly Transparent Conductors. *ACS Nano* **2011**, *5*, 9877−9882.

(25) Lin, C.-Y.; Kuo, D.-H.; Chen, W.-C.; Ma, M.-W.; Liou, G.-S. Electrical Performance of the Embedded-Type Surface Electrodes Containing Carbon and Silver Nanowires as Fillers and One-Step Organosoluble Polyimide as a Matrix. *Org. Electron.* **2012**, *13*, 2469−2473.

(26) Jung, S.; Lee, S.; Song, M.; Kim, D.-G.; You, D. S.; Kim, J.-K.; Kim, C. S.; Kim, T.-M.; Kim, K.-H.; Kim, J.-J. Extremely Flexible Transparent Conducting Electrodes for Organic Devices. *Adv. Energy Mater.* **2014**, *4*, 1−8.

(27) Chung, C.-H.; Song, T.-B.; Bob, B.; Zhu, R.; Yang, Y. Solution-Processed Flexible Transparent Conductors Composed of Silver Nanowire Networks Embedded in Indium tin Oxide Nanoparticle Matrices. *Nano Res.* **2012**, *5*, 805−814.

(28) Deng, F.; Zheng, Q.-S. An Analytical Model of Effective Electrical Conductivity of Carbon Nanotube Composites. *Appl. Phys. Lett.* **2008**, *92*, 071902.

(29) Huang, Y. Y.; Terentjev, E. M. Transparent Electrode with a Nanostructured Coating. *ACS Nano* **2011**, *5*, 2082−2089.

(30) Rao, K. D. M; Gupta, R.; Kulkarni, G. U. Fabrication of Large Area, High-Performance, Transparent conducting Electrodes using a Spontaneously Formed Crackle Network as Template. *Adv. Mater. Interfaces* **2014**, *1*, 1400090.
(31) Celle, C.; Mayousse, C.; Moreau, E.; Basti, H.; Carella, A.; Simonato, J.-P. Highly Flexible Transparent Film Heater Based on Random Networks of Silver Nanowires. *Nano Res.* **2012**, *5*, 427−433.
(32) Kang, J.; Kim, H.; Kim, K. S.; Lee, S. K.; Bae, S.; Ahn, J. H.; Kim, Y. J.; Choi, J. B.; Hong, B. H. High-Performance Graphene-Based Transparent Flexible Heaters. *Nano Lett.* **2011**, *11*, 5154−5158.